Int J Adv Manuf Technol (2017) 91:3727–3735
DOI 10.1007/s00170-017-0029-3

ORIGINAL ARTICLE

Position deviation of bending point in asymmetric V-die bending process with HSS trapezoid sheet

Daw-Kwei Leu [1]

Received: 12 September 2016 / Accepted: 9 January 2017 / Published online: 27 January 2017

Abstract The prediction of the deviation of bending point in asymmetric V-die bending is extremely needed for practical application. An analytical model and a series of experiments are performed to characterize high strength steel (HSS) sheet metal parts fabricated by asymmetric V-die bending dies and trapezoid sheet. The proposed strategy uses an elementary bending theory to develop a basic model to predict the position deviation of bending point of asymmetric V-die bending process and to test its viability for a trapezoid sheet. Accordingly, a series of experiments obtained good agreement with the calculations. The effects of die radius on deviation in the bending point were experimentally tested to identify the behavior of position deviation in sheet metal bending processes. The experimental results show the important role of contact friction on deviation change; however, its value, i.e., friction coefficient, is always difficult to be determined in calculation. In conclusion, the interactive effects of process parameters are complex and show the important roles of die radius and sheet width on deviation change. The results of this study can be considered when developing process design guidelines for asymmetric processes in HSS sheets.

Keywords HSS · Deviation · V-die bending · Trapezoid · Bending point

✉ Daw-Kwei Leu
dkleu@tpcu.edu.tw

[1] Department of Mechanical Engineering, Taipei City University of Science and Technology, No. 2, Xueyuan Road, Beitou, Taipei, Taiwan 112, Republic of China

1 Introduction

Bending of metal sheet is an essential metal-forming process in many industries, particularly the automobile industry. Bending processes are widely used to stamp structural parts such as motor vehicle bumpers. However, since springback and failure can cause major defects during sheet bending, potential improvements in this process have been studied intensively by many researchers. However, their work focused on the conventional bending which is based on the symmetrical type of dies and sheets. Although much progress has been made, further theoretical development and experimentation are needed to enable practical applications of these findings.

Because of its high strength and low cost compared to other conventional metals, high strength steel (HSS) is widely used in automotive body structures to reduce weight, which then improves energy efficiency. Recently, Bakhshi-Jooybari et al. [1] experimentally and numerically investigated how significant parameters affect springback in CK67 anisotropic steel sheets during U-die and V-die bending. Narayanasamy and Padmanabhan [2] applied response surface methodology to predict bend force during air bending process in interstitial free steel sheet. The results showed that bend force is mainly affected by punch velocity and punch radius. Farsi and Arezoo [3] investigated the adjustment of bending sequence in progressive dies for reducing the time and cost of producing complex parts. Yu [4] investigated variation of elastic modulus under plastic deformation and how it affected springback. Ramezani et al. [5] proposed a Stribeck friction model in an FE simulation to predict springback of HSS sheets in V-bending process. Ramezani and Mohd Ripin [6] applied a dry friction model, which is a function of contact area ratio and strain hardening exponent, in ABAQUS/Standard to simulate V-bending process of aluminum alloy 6061-T4 sheets.

Fu and Mo [7] numerically investigated the incremental air bending of high strength sheet metal. Ozturk et al. [8] investigated how warm temperature affected springback of titanium sheets. Fu and Mo [9] investigated springback prediction of high strength sheet metal in air bending which tool design is based on GA-BPNN. Chatti and Hermi [10] examined springback prediction based on a nonlinear recovery. Baseri et al. [11] proposed back propagation algorithm of fuzzy learning to predict springback of V-bending process. Kardes Sever et al. [12] investigated how E-modulus variation with strain affected springback in V-die bending and U-bending of advanced high strength steel AHSS-DP 780. Fu [13] applied ABAQUS FEA to investigate springback of air bending. Malikov et al. [14] experimentally and analytically investigated bending force of structured sheet metals in air bending. The results showed that bending force was significantly affected by bending position and structure location. Moreover, some effective methods applied to predict and suppress springback have been developed. Duc-Toan et al. [15] proposed a material model to predict springback of AZ31 magnesium alloy sheet in V-bending under various temperatures. Lee et al. [16] investigated how homogeneous anisotropic hardening affected springback of pre-strained U-draw/bending. Song and Yu [17] applied neural networks in a finite element method to predict springback of a T-section beam. Parsa and Mohammadi [18] investigated springback of Al3105/polypropylene/Al3105 laminates in V-die bending. Zong et al. [19] investigated springback of Ti-6Al-4V alloy sheets in hot V-bending. Fang et al. [20] investigated springback in micro V-bending with consideration of grain heterogeneity. Although much progress has been made, further theoretical development and experimentation are needed to enable practical applications of these findings.

This work investigated the asymmetric V-die bending of HSS sheet. Herein, asymmetric V-die bending is defined as the use of trapezoid sheet in which the width is various along the direction of sheet length. Figure 1 shows the asymmetric V-die bending mode with trapezoid sheet. In fact, the practical industrial demands of assembly and multi-forming in precision devices have increased the use of asymmetric bending. However, two common defects in asymmetric bending are (1) an incorrectly positioned bending point in the center part of the punch causing a difference in contact friction force and contact area on both contact sides, i.e., position deviation, and (2) a difference in width length producing a different bend angle after unloading on both sides for the different loading path and contact friction. Until now, the only practical solutions for these problems are those proposed by Leu [21, 22], who investigated the position deviation and springback of V-die bending process with asymmetric bend length [21], and with different punch and die radii on both sides [22], respectively.

This study performed analytical modeling with elementary bending theory and a series of experiments to clarify basic characteristics of HSS sheet during asymmetric V-die bending with trapezoid sheet. To enable practical application, a major objective is precisely controlling the position of bending point to satisfy the production demand identically. This work focused on how die corner radius affects the position deviation of bending point. The experiments show that the considered die radii affect position deviation of bending point in different ways and show the important role of contact friction on deviation change. The findings of this study can be used to establish guidelines for designing tools for stamping of HSS sheets. Accordingly, this study also proposes methods of minimizing these defects to obtain a precise asymmetric bent component.

2 Materials and methods

In this study, a proposed model, based on an elementary bending theory, is developed to predict position deviation of bending point in asymmetric V-die bending process with trapezoid sheet. The HSS sheets of SPFC 440 sheet metal of JIS G3135 are taken with thickness 1.0 mm for experiments.

Based on the middle line along the sheet length in thickness direction shown in Fig. 2, the parameters of tool geometry used to modeling asymmetric V-die bending with trapezoid sheet are defined as $\rho \equiv \rho + t/2$, $\rho_1 \equiv \rho_1 + t/2$, and $\rho_2 \equiv \rho_2 + t/2$, where $\rho \equiv \mathrm{Rp}$ is the radius of punch head, $\rho_1 \equiv \mathrm{Rd1}$ is the radius of die corner on the left-hand side, $\rho_2 \equiv \mathrm{Rd2}$ is the radius of die corner on the right-hand side, t is sheet thickness, and b_1 and b_2 are the width of trapezoid sheet on the left-hand and right-hand sides, respectively.

In this study, the proposed model is shown in Fig. 2 and the mechanical properties of sheet material are shown in Table 1. According to the deformation characteristics of asymmetric V-die bending, the total deformation energy of final bent part can be divided into three kinds of deformed energy. During the bending process, the bending moment acting on bent part induced bending energy. When the bending point moves to the left-hand side on the surface of punch head, a reverse moment (re-bending) due to the initial bent sheet with punch radius ρ is re-bent to straight of the bent sheet. The second kind of deformed energy is due to the movement of bending point along the direction of sheet length. The third kind of deformed energy is due to the contact friction force along the direction of sheet length on the surface of punch head. For simplicity, the sheet thickness is assumed constant during bending. Both edges of the sheet are simply straight without deformation because the end of the sheet is free and rotates around the die corner freely.

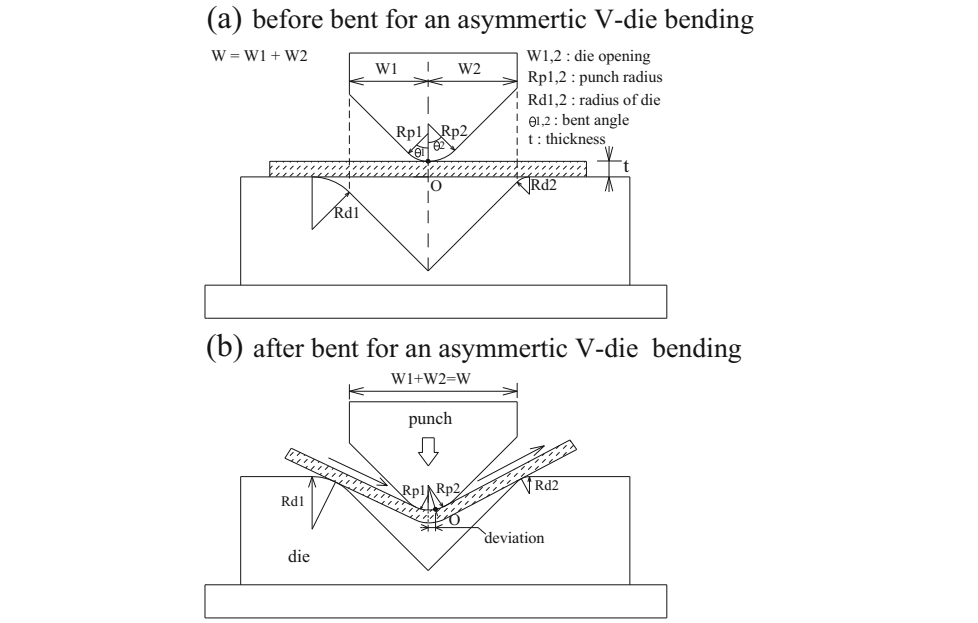

Fig. 1 Scheme of **a** asymmetric V-die bending [21, 22] and $Rp_1 = Rp_2 = Rp$ ($\theta_1 = \theta_2 = \theta$) herein, **b** position deviation of bending point [21, 22], and **c** successive bending processes during asymmetric V-die bending with trapezoid sheet

2.1 Deformation energy due to bending moment

Based on the proposed model shown in Fig. 2, the deformation energy W_b due to bending effect can be simplified as follows:

$$W_b = \int M d\theta = \int M \frac{ds}{\rho} \cong \int M \frac{dx}{\rho} = \frac{1}{\rho}\int_{x_1}^{x_2}(m_1 x + m_2)dx + \frac{2}{\rho}\int_{x_2}^{x_2^0}(m_1 x + m_2)dx$$
$$= \frac{1}{\rho}\left[\left(m_1\frac{x^2}{2} + m_2 x\right)\Big|_{x_1}^{x_2} + 2\left(m_1\frac{x^2}{2} + m_2 x\right)\Big|_{x_2}^{x_2^0}\right] \quad (1)$$

where ρ is punch head radius. The second term of the integral shows the effect of re-bending induced by the movement of bending point. Accordingly, M is bending moment, which is a linear function of position x due to the asymmetric shape of trapezoid sheet with a linear relationship in sheet width,

$$M = m_1 x + m_2 \quad (2)$$

where m_1 and m_2 are based on the work by Leu [23],

$$m_1 = \frac{kbt^2}{4(1+n)}\left(\frac{1+R}{\sqrt{1+2R}}\right)^{1+n}\left(\frac{t}{2\rho}\right)^n \frac{b_2 - b_1}{l_0} \quad (3)$$

$$m_2 = \frac{kbt^2}{4(1+n)}\left(\frac{1+R}{\sqrt{1+2R}}\right)^{1+n}\left(\frac{t}{2\rho}\right)^n b_1 \quad (4)$$

where R is normal anisotropy, and b_1 and b_2 are sheet width at positions of x_1 and x_2, respectively. Herein, the symbol Δ is defined as the amount of position deviation of bending point.

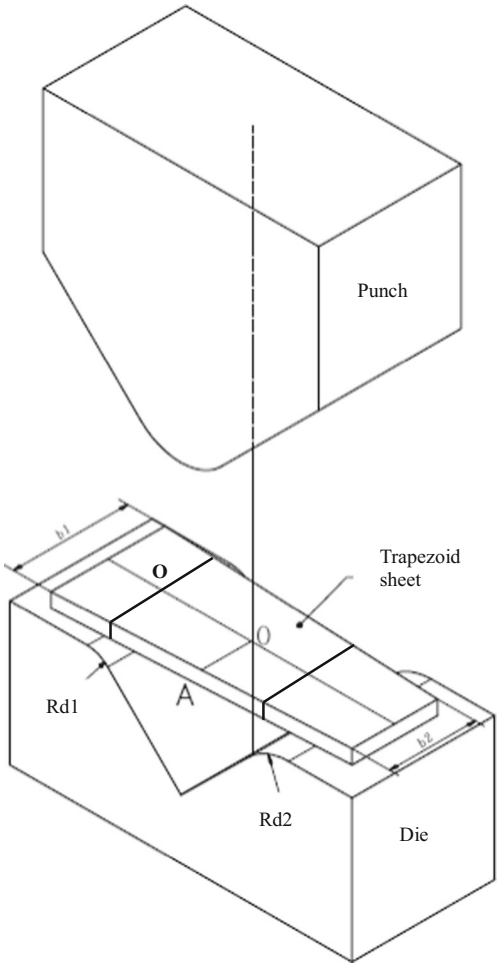

Fig. 2 The model of asymmetric V-die bending model in which a position deviation of bending point will occur

Then, positions x_1 and x_2 along the sheet length show the positions of material element on the arc part of punch head, in which x_1 shows the element position on the left-hand side and x_2 shows the element position on the right-hand side, at the final stage of bending,

$$x_1 = \rho_1 \sin\theta + W_1 - \rho\theta - \Delta \tag{5}$$

$$x_2 = \rho_1 \sin\theta + W_1 + \rho\theta - \Delta \tag{6}$$

The angle θ is the half of bend angle and the length l_0 shows the distance between the left-hand and the right-hand corners on die surface,

$$l_0 = (\rho_1 + \rho_2)\sin\theta + W \tag{7}$$

Positions x_1^o and x_2^o show the initial element positions on the arc of punch head on the left-hand and right-hand sides at the final stage without deviation,

$$x_1^o = \rho_1 \sin\theta + W_1 - \rho\theta \tag{8}$$

$$x_2^o = \rho_1 \sin\theta + W_1 + \rho\theta \tag{9}$$

The width of punch head at the left-hand side is W_1

$$W_1 = \frac{1}{2}\left[W - \frac{(\rho_1 - \rho_2)(1-\cos\theta)}{\tan\theta}\right] \tag{10}$$

Then, the deformation energy due to bending moment can be rewritten as

$$\begin{aligned} W_b &= \frac{2\rho\theta}{\rho}\left[m_1(\rho_1\sin\theta + W_1 - \Delta) + m_2\right] + \frac{2}{\rho}\left[m_1\left(\rho_1\sin\theta + W_1 + \rho\theta - \frac{\Delta}{2}\right)\Delta + m_2\Delta\right] \\ &= -\frac{1}{\rho}m_1\Delta^2 + \frac{2}{\rho}m_2\Delta + 2\left(\frac{1}{\rho}\Delta + \theta\right)m_1(\rho_1\sin\theta + W_1) + 2\theta m_2 \end{aligned} \tag{11}$$

Accordingly, the increment of deformation energy of bending with deviation Δ is

$$\frac{\delta W_b}{\delta\Delta} = \frac{2}{\rho}\left[m_1(\rho_1\sin\theta + W_1) + m_2\right] - \frac{2}{\rho}m_1\Delta \tag{12}$$

Table 1 Material properties of SPFC 440 sheet (JIS G3135) manufactured by China Steel Company

JIS G3135 SPFC 440	Thickness t (mm)	E (GPa)	ν	σ_y (MPa)	K (MPa)	n
	1.0	205	0.3	304.7	767.5	0.231

K strength of coefficient, n work hardening coefficient, E Young's modulus, ν Poisson's ratio, σ_y yield strength, $\sigma_e = 767.5\varepsilon_p^{0.231}$ MPa

2.2 The deformation energy due to the movement of bending point

Due to the asymmetric shape of trapezoid sheet, the bending point would move on the surface of punch head by stretching force in the direction of sheet length. Then, the deformation energy due to the movement of bending point can be simplified as follows:

$$W_\Delta = \int \sigma_\theta t \mathrm{d}b\Delta = \sigma_\theta t\Delta \int \mathrm{d}b = \sigma_\theta t\Delta \int \frac{b_2-b_1}{l_0}\mathrm{d}x = \sigma_\theta t\Delta \frac{b_2-b_1}{l_0}\left(\int_{x_1}^{x_2}\mathrm{d}x + 2\int_{x_2}^{x_2^0}\mathrm{d}x\right) \tag{13}$$

where σ_θ is the circumferential stress based on the work by Leu [23] and db is the increment of width along the sheet length,

$$\sigma_\theta = \left(\frac{1+R}{\sqrt{1+2R}}\right)^{1+n}\left(\frac{t}{2\rho}\right)^n \frac{k}{1+n} \tag{14}$$

$$b = \frac{b_2-b_1}{l_0}x + b_1 \quad \text{and} \quad \mathrm{d}b = \frac{b_2-b_1}{l_0}\mathrm{d}x \tag{15}$$

where the width b along the length is a function of x based on the linear relation of trapezoid sheet in width. In Eq. (13), the second term of integral shows the effect of re-bending. Then the deformation energy due to the movement of bending point caused by stretch force can be rewritten as

$$W_\Delta = \sigma_\theta t\Delta \frac{b_2-b_1}{l_0}2\rho\theta + 2\sigma_\theta t \frac{b_2-b_1}{l_0}\Delta^2 = 2\sigma_\theta t\Delta \frac{b_2-b_1}{l_0}(\rho\theta+\Delta) \tag{16}$$

Then, the increment of deformation energy of the movement of bending point with deviation Δ is

$$\frac{\delta W_\Delta}{\delta\Delta} = 2\sigma_\theta t \frac{b_2-b_1}{l_0}(\rho\theta + 2\Delta) \tag{17}$$

2.3 The deformation energy due to friction effect

Due to the contact friction, the friction force would be induced on the contact surface of punch head along the direction of sheet length. The friction in the contact zone between workpiece and tool is a key factor in the deformation process. The friction state is described by the Coulomb friction law. The deformation energy due to friction can be simplified as follows:

$$\begin{aligned} W_\mu &= \int \mu p b \mathrm{d}s\Delta \cong \mu p\Delta \int b\mathrm{d}x = \mu p\Delta \int \left(\frac{b_2-b_1}{l_0}x + b_1\right)\mathrm{d}x \\ &= \mu p\Delta\left[\int_{x_1}^{x_2}\left(\frac{b_2-b_1}{l_0}x+b_1\right)\mathrm{d}x + 2\int_{x_2}^{x_2^0}\left(\frac{b_2-b_1}{l_0}x+b_1\right)\mathrm{d}x\right] \\ &= \mu p\Delta\left[\left(\frac{b_2-b_1}{2l_0}x^2+b_1x\right)\Big|_{x_1}^{x_2} + 2\left(\frac{b_2-b_1}{2l_0}x^2+b_1x\right)\Big|_{x_2}^{x_2^0}\right] \end{aligned} \tag{18}$$

where μ is friction coefficient on contact surface and $p = \frac{\sigma_\theta t}{\rho_i}$ is the normal pressure on the contact surface in which ρ_i is inner radius of bending which equals punch radius ρ herein. Then the deformation energy due to the contact friction force can be written as

$$\begin{aligned} W_\mu = &-\mu p \frac{b_2-b_1}{l_0}\Delta^3 \\ &+ 2\mu p\left[\frac{b_2-b_1}{l_0}(\rho_1\sin\theta + W_1) + b_1\right]\Delta^2 \\ &+ 2\mu p\rho\theta\left[\frac{b_2-b_1}{l_0}(\rho_1\sin\theta + W_1) + b_1\right]\Delta \end{aligned} \tag{19}$$

Moreover, the increment of deformation energy of friction with deviation Δ is

$$\begin{aligned} \frac{\delta W_\mu}{\delta\Delta} = &-3\mu p \frac{b_2-b_1}{l_0}\Delta^2 \\ &+ 4\mu p\left[\frac{b_2-b_1}{l_0}(\rho_1\sin\theta + W_1) + b_1\right]\Delta \\ &+ 2\mu p\rho\theta\left[\frac{b_2-b_1}{l_0}(\rho_1\sin\theta + W_1) + b_1\right] \end{aligned} \tag{20}$$

2.4 A stationary value problem of asymmetric V-die bending with trapezoid sheet

From Sections 2.1 to 2.3, the total deformation energy of asymmetric V-die bending with trapezoid sheet can be simply written as follows:

$$W = W_b + W_\Delta + W_\mu \tag{21}$$

The total deformation energy W is a stationary value. Therefore, the increment of W with deviation Δ should be vanished, i.e.,

$$\frac{\delta W}{\delta\Delta} = \frac{\delta W_b}{\delta\Delta} + \frac{\delta W_\Delta}{\delta\Delta} + \frac{\delta W_\mu}{\delta\Delta} = 0 \tag{22}$$

Then, Eq. (22) can be reduced as an equation with one unknown quantity Δ and two orders,

$$\begin{aligned}\frac{\delta W}{\delta \Delta} &= \left(-3\mu p\frac{b_2-b_1}{l_0}\right)\Delta^2+\left\{-\frac{2}{\rho}m_1+4\sigma_\theta t\frac{b_2-b_1}{l_0}+4\mu p\left[\frac{b_2-b_1}{l_0}(\rho_1\sin\theta+W_1)+b_1\right]\right\}\Delta \\ &+\left\{\frac{2}{\rho}[m_1(\rho_1\sin\theta+W_1)+m_2]+2\sigma_\theta t\frac{b_2-b_1}{l_0}\rho\theta+2\mu p\rho\theta\left[\frac{b_2-b_1}{l_0}(\rho_1\sin\theta+W_1)+b_1\right]\right\} \\ &= A\Delta^2+B\Delta+C=0\end{aligned} \tag{23}$$

The position deviation Δ in Eq. (23) can be easily calculated by a solution equation under the constants of A, B, and C. The solution equation is as follows:

$$\Delta=\frac{-B\pm\sqrt{B^2-4AC}}{2A} \quad \text{and say} \quad \Delta=\mathrm{MIN}\left\{\left|\frac{-B+\sqrt{B^2-4AC}}{2A}\right|,\ \left|\frac{-B-\sqrt{B^2-4AC}}{2A}\right|\right\} \tag{24}$$

where

$$\begin{aligned}A &= \left(-3\mu p\frac{b_2-b_1}{l_0}\right) \\ B &= \left\{-\frac{2}{\rho}m_1+4\sigma_\theta t\frac{b_2-b_1}{l_0}+4\mu p\left[\frac{b_2-b_1}{l_0}(\rho_1\sin\theta+W_1)+b_1\right]\right\} \\ C &= \left\{\frac{2}{\rho}[m_1(\rho_1\sin\theta+W_1)+m_2]+2\sigma_\theta t\frac{b_2-b_1}{l_0}\rho\theta+2\mu p\rho\theta\left[\frac{b_2-b_1}{l_0}(\rho_1\sin\theta+W_1)+b_1\right]\right\}\end{aligned}$$

Equation (24) is used to calculate the position deviation of bending point in asymmetric V-die bending process with trapezoid sheet. Obviously, the relation between position deviation and process parameters seems complex.

3 Experiment, results, and discussion

Figure 2 shows the asymmetric V-die bending model used in the experiment. A friction coefficient of $\mu=0.15$ is assumed based on the use of WD-40 mineral oil in the experiment. The material used in the experiments was SPFC 440 of JIS G3135 with thickness t = 1.0 mm. Table 1 shows its mechanical properties. The rim of the sheet was polished to remove irregularities and to obtain a smooth surface. Table 2 shows the dimensions of the experimental tools (total four sets). The experimental values and calculated data of deviation for four die sets are shown in Table 3. The experiments were performed with a 300-kN hydraulic test machine, and optical equipment was used to record the deviation in the bending point. Each experiment was carried out three times. The deviation is defined as the arc length measured in middle line along the sheet length. Figure 3 shows the experimental tools for asymmetric V-die bending with trapezoid sheet and the occurrence of deviation of bending point in experiments.

3.1 Verification of the proposed model

Figure 4 and Table 3 show the comparison of deviation Δ between experiment and calculation for the four experimental tools shown in Table 2. The proposed model was verified by comparing the calculated values with the experimental results. The errors (the difference between calculation and experiment) shown in Fig. 4 and Table 3 are acceptable under the

Table 2 Experimental conditions and geometric dimensions of dies

	ρ_1	ρ_2	b_1	b_2	l_0
R6-R3	6	3	41.70	19.15	56.363
R3-R6	3	6	40.85	18.30	56.363
R6-R6	6	6	41.70	18.30	58.484
R3-R3	3	3	40.85	19.15	54.242

ρ_1, die corner radius on the left-hand side; ρ_2, die corner radius on the right-hand side; lubricant: WD-40 mineral oil; surface roughness as received; radius of punch head $\rho=5.0$ mm; half of bend angle $\theta=45$; punch speed set to 1 mm/min

Table 3 Experimental results and calculated values of position deviation Δ

Dev (Δ)	Exp	Cal (μ = 0.15)	Error (Cal − Exp)	Best μ	Dev of best μ
R6-R3	3.4	3.674	0.274	0.17	3.381
R3-R6	2.9	3.693	0.793	0.24	2.904
R6-R6	3.2	3.684	0.484	0.19	3.191
R3-R3	2.7	3.682	1.082	0.31	2.700

Ra-Rb: Ra (at the left-hand side of "Ra-Rb") indicates the radius of die corner in the left-hand side; Rb (at the right-hand side of "Ra-Rb") indicates the radius of die corner in the right-hand side (for example, the case of R6-R3 indicates that R6, the radius of die corner in the left-hand side, is 6 mm and R3, the radius of die corner in the right-hand side, is 3 mm); *Exp* experimental data of Δ; *Cal* calculated value of Δ; Error: difference between calculation and experiment (=Cal − Exp); *Dev* position deviation of bending point, Δ; lubricant: WD-40 mineral oil

assumption of μ = 0.15 for the practical purpose. The deviation errors ranged from 0.27 to 1.08 in all cases. The large error of case R3-R3 in Table 3 may result from an improper surface condition as carrying out the experiment of case R3-R3. Notably, the position deviation was significantly affected by surface friction. The friction clearly has an important effect on deviation change. Table 3, however, shows fairly good agreement between the calculation results and the experimental results. Furthermore, the best friction coefficient to approach the experimental result was carried out to examine the variation of friction effect, which is shown in Table 3. The largest value of friction coefficient was the case of R3-R3 (μ = 0.31) and the smallest friction coefficient was the case of R6-R3 (μ = 0.17). The friction forces are increased on small die corner radius where severe plastic deformation conditions occurred, which may change the surface condition and then reduce the sliding of bending point on the contact surface. The range of friction coefficient seems reasonable for the surface condition of sheet which surface conditions were as received. Clearly, lubrication (friction effect) substantially affects the amount of deviation, and its value, i.e., friction coefficient, is always difficult to be determined in calculation. Further study of friction effect on deviation change is necessary.

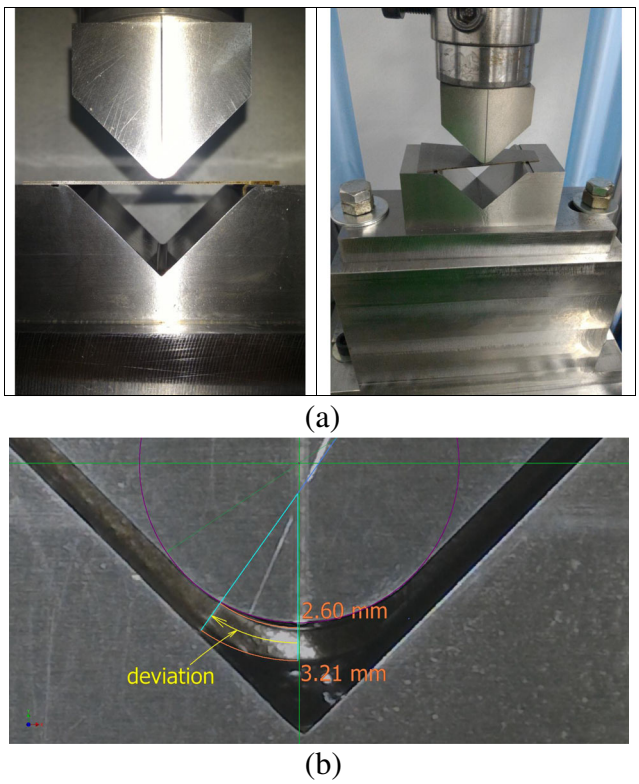

Fig. 3 **a** Experimental tools for asymmetric V-die bending with HSS trapezoid sheet and **b** the occurrence of deviation Δ in experiments: outer surface, Δ = 3.21; inner surface, Δ = 2.60 mm

3.2 Effects of die radius on deviation

Figure 5 shows how die radius affects position deviation. Case 1 (compare R6-R3 with R3-R6) shows that deviation of R6-R3 (R6 at the left-hand side of "R6-R3" is the die radius on the left-hand side of die and R3 at the right-hand side of "R6-R3" is the die radius on the right-hand side of die) is larger than that of R3-R6 (R3 is the die radius on the left-hand side of die and R6 on the right-hand side of die). This effect may result from the increased movement on the side with the large die radius, which causes the material element moving on the surface with

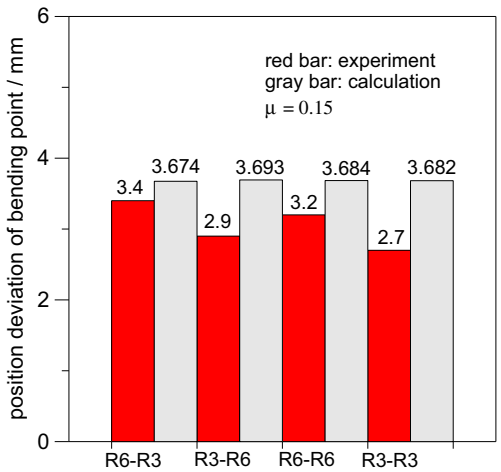

Fig. 4 Comparison between experimental results and calculated values for the four cases shown in Table 2 (cases of R6-R3, R3-R6, R6-R6, and R3-R3)

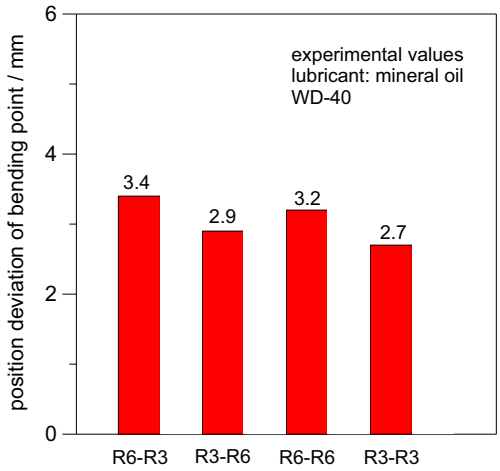

Fig. 5 Experimental values for deviation obtained under the cases of Table 2

large radius easily and then induced a large deviation of bending point. Case 2 (compare R6-R3 with R6-R6) shows that deviation of R6-R3 (R6 is the die radius on the left-hand side of die and R3 on the right-hand side of die) is larger than that of R6-R6 (a symmetric die with die corner radius R6 on both sides). This effect may result from the increased resistance of movement on the side with the small corner radius in asymmetric die (on the right-hand side of R6-R3); on the other side, the large corner radius increases the movement of material element on the surface. Then the difference of corner radius in asymmetric die induced a larger deviation than that of die with the same corner radius (symmetric die). Case 3 (compare R6-R3 with R3-R3) shows that deviation of R6-R3 (R6 is the die radius on the left-hand side of die and R3 on the right-hand side of die) is larger than that of R3-R3 (a symmetric die with die corner radius R3 on both sides). This effect results from the same reason of case 2. Notably, the symmetric die with small radius will significantly increase resistance of movement which is larger than that with large die radius. Case 4 (compare R6-R6 with R3-R6) shows that deviation of R6-R6 (a symmetric die with die corner radius R6 on both sides) is larger than that of R3-R6 (R3 is the die radius on the left-hand side of die and R6 on the right-hand side of die). A converse effect occurs, which is different from the results of case 3. A complex interaction occurs and shows that sheet width apparently counteracts the effect of die radius on deviation. This effect may result from the increased movement of bending point on the side with large width and small die radius, which then counteracts the movement of bending point caused by the small width on the other side. Then this effect induced a small deviation in bending point. Case 5 (compare R3-R6 with R3-R3) shows that deviation of R3-R6 (R3 is the die radius on the left-hand side of die and R6 on the right-hand side of die) is slightly larger than that of R3-R3 (a symmetric die with die corner radius R3 on both sides). This effect may result from the same reason of case 4. Moreover, the effect of large width and small die radius positioned on the same side seems to decrease the amount of deviation. Case 6 (compare R6-R6 with R3-R3) shows that deviation of R6-R6 (a symmetric die with die corner radius R6 on both sides) is larger than that of R3-R3 (a symmetric die with die corner radius R3 on both sides). This effect results from the increased movement of material element on the side with the large die radius, which causes the material element to move on the surface with large radius easily. In general, the large difference in sheet width between left-hand and right-hand sides increases the amount of movement of material element and then induced a large deviation in bending point. These interactive effects show the important roles of die radius and sheet width on deviation change.

The analysis shows that the interaction of process parameters is very complex and irregular. The process parameters cannot be considered in isolation. Therefore, further studies are needed to elucidate complex interactions among process parameters.

4 Conclusions

This pioneering work in the use of asymmetric tools to analyze asymmetric V-die bending process with trapezoid sheet yielded the following findings:

1. Deviation calculation: A simplified model is proposed based on an elementary bending theory and total plastic deformation theory in order to predict the position deviation of bending point in asymmetric V-die bending process with trapezoid sheet. Experiments verify its viability for practical use. This model is a function of various process parameters, such as material mechanical property, sheet width, contact friction, and die geometry, and the interactions are complex among process parameters. The experimental results show the important role of contact friction on deviation change; however, its value, i.e., friction coefficient, is always difficult to be determined in calculation.
2. Deviation experiment: The effect of die radius on position deviation is examined and its relation is complex. (1) The increased movement on the side with the large corner radius of die causes the material element moving on the surface with large radius easily and then induced a large deviation of bending point. (2) Moreover, the increased resistance of movement on the side with the small corner radius increases the movement of material element on the other side with large corner radius and then induced a larger deviation of bending point, which is larger than that of symmetric die with same die radii on both sides. (3) Then, the symmetric die with small radius will significantly increase resistance of movement, and this resistance of

movement is larger than that of the symmetric die with large die radius. (4) A converse effect occurs that sheet width apparently counteracts the effect of die corner radius on deviation. This effect may result from the increased movement on the side with large sheet width and small die radius, which counteracts the movement of material element that is caused by the small width on the other side. Then this effect induced a small deviation of bending point. (5) Moreover, the effect of large sheet width and small die radius on one side seems to decrease the amount of deviation of bending point. (6) In general, the large difference in sheet width between the left-hand and the right-hand sides of sheet increases the amount of movement of material element and then induced a large deviation of bending point. These interactive effects are complex and show the important roles of die corner radius and sheet width on deviation change.

In conclusion, the effects of process parameters on deviation vary. Therefore, this study indicates that the interaction of process parameters is very complicated and irregular. The process parameters cannot be considered in isolation.

Acknowledgements The author would like to thank the Ministry of Science and Technology of the Republic of China, Taiwan for financially supporting this research under Contract No. MOST 104-2221-E-149-004. Z.-C. Chen, B.-Y. Chen, Y.-C. Chen, J.-G. Lin, and Y.-Y. Zhan are appreciated for their helpful discussions.

References

1. Bakhshi-Jooybari M, Rahmani B, Daeezadeh V, Gorji A (2009) The study of spring-back of CK67 steel sheet in V-die and U-die bending processes. Mater Des 30(7):2410–2419
2. Narayanasamy R, Padmanabhan P (2009) Application of response surface methodology for predicting bend force during air bending process in interstitial free steel sheet. Int J Adv Manuf Technol 44: 38–48
3. Farsi MA, Arezoo B (2009) Development of a new method to determine bending sequence in progressive dies. Int J Adv Manuf Technol 43:52–60
4. Yu HY (2009) Variation of elastic modulus during plastic deformation and its influence on springback. Mater Des 30:846–850
5. Ramezani M, Mohd Ripin Z, Ahmad R (2010) Modelling of kinetic friction in V-bending of ultra-high-strength steel sheets. Int J Adv Manuf Technol 46:101–110
6. Ramezani M, Mohd Ripin Z (2010) A friction model for dry contacts during metal-forming processes. Int J AdvManuf Technol 51: 93–102
7. Fu Z, Mo J (2010) Multiple-step incremental air-bending forming of high-strength sheet metal based on simulation analysis. Mater Manuf Process 25(8):808–816
8. Ozturk F, Ece RE, Polat N, Koksal A (2010) Effect of warm temperature on springback compensation of titanium sheet. Mater Manuf Process 23(9):1021–1024
9. Fu Z, Mo J (2011) Springback prediction of high-strength sheet metal under air bending forming and tool design based on GA–BPNN. Int J Adv Manuf Technol 53(5–8):473–483
10. Chatti S, Hermi N (2011) The effect of non-linear recovery on springback prediction. Comput Struct 89(13–14):1367–1377
11. Baseri H, Bakhshi-Jooybari M, Rahmani B (2011) Modeling of spring-back in V-die bending process by using fuzzy learning back-propagation algorithm. Expert Syst Appl 38(7):8894–8900
12. Kardes Sever N, Mete OH, Demiralp Y, Choi C, Altan T (2012) Springback prediction in bending of AHSS-DP 780. Proc NAMRI/SME 40:1–10
13. Fu ZM (2012) Numerical simulation of springback in air-bending forming of sheet metal. Appl Mech Mater 121–126:3602–3606
14. Malikov V, Ossenbrink R, Viehweger B, Michailov V (2012) Experimental investigation and analytical calculation of the bending force for air bending of structured sheet metals. Adv Mater Res 418–420:1294–1300
15. Duc-Toan N, Seung-Han Y, Dong-Won J, Tien-Long B, Young-Suk K (2012) A study on material modeling to predict spring-back in Vbending of AZ31 magnesium alloy sheet at various temperatures. Int J Adv Manuf Technol 62:551–562
16. Lee JY, Lee JW, Lee MG, Barlat F (2012) An application of homogeneous anisotropic hardening to springback prediction in pre-strained U-draw/bending. Int J Solids Struct 49(25):3562–3572
17. Song Y, Yu Z (2013) Springback prediction in T-section beam bending process using neural networks and finite element method. Archives of Civil and Mechanical Engineering 13(2):229–241
18. Parsa MH, Mohammadi SV (2014) Al3105/polypropylene/Al3105 laminates springback in V-die bending. Int J Adv Manuf Technol 75(5):849–860
19. Zong YY, Liu P, Guo B, Shan DB (2015) Springback evaluation in hot v-bending of Ti-6Al-4V alloy sheets. Int J Adv Manuf Technol 76(1):577–585
20. Fang Z, Jiang ZY, Wei DB (2015) Study on springback in micro V-bending with consideration of grain heterogeneity. Int J Adv Manuf Technol 78(5):1075–1085
21. Leu DK (2013) Position deviation in V-die bending process with asymmetric bend length. Int J Adv Manuf Technol 64:93–103
22. Leu DK (2015) Position deviation of bending point in V-die bending process with asymmetric dies. Int J Adv Manuf Technol 79: 1095–1108
23. Leu DK (1997) A simplified approach for evaluation bendability and springback in plastic bending of anisotropic sheet metals. J Mater Process Technol 66:9–17